# Estimating soil hydraulic parameters from transient flow experiments in a centrifuge using parameter optimization technique

Jirka Šimůnek

Department of Environmental Sciences, University of California, Riverside, California, USA

John R. Nimmo

U.S. Geological Survey, Menlo Park, California, USA

Received 28 May 2004; revised 20 January 2005; accepted 7 February 2005; published 27 April 2005.

[1] A modified version of the Hydrus software package that can directly or inversely simulate water flow in a transient centrifugal field is presented. The inverse solver for parameter estimation of the soil hydraulic parameters is then applied to multirotation transient flow experiments in a centrifuge. Using time-variable water contents measured at a sequence of several rotation speeds, soil hydraulic properties were successfully estimated by numerical inversion of transient experiments. The inverse method was then evaluated by comparing estimated soil hydraulic properties with those determined independently using an equilibrium analysis. The optimized soil hydraulic properties compared well with those determined using equilibrium analysis and steady state experiment. Multirotation experiments in a centrifuge not only offer significant time savings by accelerating time but also provide significantly more information for the parameter estimation procedure compared to multistep outflow experiments in a gravitational field.

**Citation:** Šimůnek, J., and J. R. Nimmo (2005), Estimating soil hydraulic parameters from transient flow experiments in a centrifuge using parameter optimization technique, *Water Resour. Res.*, *41*, W04015, doi:10.1029/2004WR003379.

## 1. Introduction

[2] The main information needed for evaluating, analyzing, and predicting flow and solute transport in soils concerns the soil hydraulic properties. Traditional methods of measuring soil hydraulic properties are tedious and time consuming [*Dane and Topp*, 2002]; therefore faster, easier techniques are constantly being sought [e.g., *Hopmans et al.*, 2002]. One way of accelerating the measurement process is by carrying out needed experiments in a centrifuge. The steady state conditions required for many types of measurements can be achieved in much shorter time [e.g., *Nimmo et al.*, 1987, 2002; *Nimmo and Mello*, 1991; *Conca and Wright*, 1992].

[3] Over the last century, high-speed centrifuges have become standard in scientific and technical fields of soil physics, petroleum industry and environmental engineering for measuring water contents, and saturated and unsaturated hydraulic conductivities. *Briggs and McLane* [1907] used a centrifuge to measure what they called the ''moisture equivalent,'' a single-number index of a soil's capacity to retain water. Later, the water retention curve was the measurement objective, for example, in the work of *Gardner* [1937], *Russell and Richards* [1938], and *Hassler and Brunner* [1945]. In these methods the water in an unsaturated sample equilibrates with the centrifugal field, much as in the hanging-column method [*Dane and Hopmans*, 2002] it equilibrates with a gravitational field. Development of such techniques has continued to the present [*Forbes*, 1994; *Paningbatan*, 1980; *Sigda and Wilson*, 2003]. The use of centrifuge-scaled physical modeling of dynamic unsaturated flow has also been explored recently [e.g., *Culligan et al.*, 1997; *Nakajima et al.*, 2003]. For measuring unsaturated hydraulic conductivity by the steady state centrifuge method, two different types of apparatus have been used, as explained by *Nimmo et al.* [2002]. In the internal flow control (IFC) apparatus the means of controlling flow is internal to the centrifuge bucket [*Nimmo et al.*, 1987], while in the unsaturated flow apparatus (UFA), the flow is controlled outside the centrifuge [*Conca and Wright*, 1992, 1998]. Each of these implementations has its own advantages and disadvantages, for example larger samples and greater speeds with the IFC apparatus, faster operation and less demand on the operator with the UFA apparatus [*Nimmo et al.*, 2002]. Some experiments have investigated transient instead of steady flow [e.g., *Alemi et al.*, 1976; *Nimmo*, 1990], and even unstable flow [*Culligan et al.*, 1997; *Griffioen et al.*, 1997]. So far these transient methods have not led to widely used techniques for soil property measurement, though they provide significant insights into the nature of unsaturated flow.

[4] Recent advances allow measurement of state variables inside the rotating sample. *Nimmo* [1990] measured electrical conductivity using a four-electrode technique and converted the measured values into water contents. *Savvidou and Culligan* [1998] monitored pore pressures and solute concentrations in a spinning sample with miniature pressure


0043-1397/05/2004WR003379$09.00

transducers and resistivity probes. Investigators at the Idaho National Engineering and Environmental Laboratory are experimenting with measuring pressure heads using miniature tensiometers rotating together with soil samples [*Mattson et al.*, 2003].

[5] Direct solvers of the Richards equation modified to account for a centrifugal field have been developed in the last two decades. *Bear et al.* [1984] presented a theory of fluid flow through a deformable porous medium in the presence of a centrifugal force and then solved the resulting flow and deformation equations using the finite difference method. They discussed implementation of several types of boundary conditions for different applications and presented calculated water content and pressure head profiles for hypothetical simulations. In their simulations they showed that the porosity changes were less than 0.01% after 12 minutes of centrifuging, and thus can be neglected in majority of applications. *Nimmo* [1990] also developed a direct solver of the Richards equation for a centrifugal field and successfully compared numerical simulations using independently determined soil hydraulic properties to measured results of transient flow experiments.

[6] An alternative to steady state experiments is analysis of transient experiments using parameter estimation techniques [*Hopmans et al.*, 2002]. Steady state calculations are often based on assumption of constant water contents and zero, or linear, pressure head gradients, which is not always the case. On the other hand, parameter estimation techniques, such as those based on the numerical solution of the Richards equation, do not require such assumptions, and are constrained only by assumptions inherent in the derivation of the transient Richards equation. The one-step outflow method [*Gardner*, 1956; *Kool et al.*, 1985] and the multistep outflow method [*van Dam et al.*, 1994; *Eching and Hopmans*, 1993; *Durner et al.*, 1999] are frequently used in combination with a parameter estimation technique to determine soil hydraulic parameters in a gravitational field [*Hopmans et al.*, 2002]. During the experiment, pressures or suctions are applied at the top or bottom of the soil sample while the resulting outflow from the sample, and, optionally, also the pressure head within the sample, are measured. Cumulative outflow data in combination with measured pressure heads, if available, are then used to define the objective function against which the numerical model is calibrated to estimate soil hydraulic parameters.

[7] Similar procedures can be followed in the centrifuge using step changes in rotational speed rather than applied pressure head. Different rotation speeds then, when the lower boundary condition is specified by the zero pressure level at an imposed water table established within a porous plate below the soil boundary, will result in different suctions applied at the bottom of the sample. Similarly to the multistep outflow experiment in a gravitational field, sequentially increasing rotational speeds will result in stepwise draining of the sample. This information can be used to define the objective function for model calibration. *Alemi et al.* [1976] presented a theory for analyzing the volumetric outflow of water from a soil core when the speed of centrifugation is suddenly increased. Their approach, however, was not based on numerical inversion of the Richards equation, and they did not present or analyze experimental data.

[8] When a multistep outflow experiment in a gravitational field is carried out for a long enough time at each pressure step to reach steady conditions, the resulting pairs of water contents and pressure heads define data points of the retention curve. Similar experiments in a centrifugal field can provide much more information. Since a centrifugal field results in pressure heads that vary greatly between the top and bottom of the sample, each steady state condition can provide multiple data points of the retention curve depending on the number of positions at which the water content is measured.

[9] In this manuscript we address the question of whether one can obtain additional benefits by combining the advantages of centrifuge-accelerated experiments with parameter estimation analysis. The objectives of this paper are threefold. The first is to present direct and inverse solvers of the Richards equation modified for a transient centrifugal field. Second, to apply the inverse solver for parameter estimation of the soil hydraulic parameters using multirotation transient flow experiments in a centrifuge. Third, to evaluate the method by comparing estimated soil hydraulic properties with those determined independently using an equilibrium analysis.

## 2. Theory

### 2.1. Mathematical Model

[10] Darcy-Buckingham's law for one-dimensional flow in a centrifugal field, neglecting gravity and hysteresis, can be expressed as [*Nimmo et al.*, 1987; *Conca and Wright*, 1992]

$$q = -K^*(\psi)\left(\frac{d\psi}{dr} - \rho\omega^2 r\right) \tag{1}$$

where $q$ is the Darcy flux [$LT^{-1}$], $\psi$ is the matric potential [$ML^{-1}\,T^{-2}$, Pa], $\rho$ is the bulk density of water [$ML^{-3}$], $\omega$ is the angular speed [$radT^{-1}$], $K^*$ is the hydraulic conductivity [$L^3TM^{-1}$], and $r$ is the radial coordinate [L]. This formulation leads to units for the hydraulic conductivity that are not often used. Simple transformation of the equation leads to conductivity being expressed in more commonly used units of [$LT^{-1}$] and Darcy-Buckingham's law being expressed in terms of the pressure head:

$$q = -K^*\rho g\left(\frac{d\psi}{\rho g dr} - \frac{\rho\omega^2 r}{\rho g}\right) = -K\left(\frac{dh}{dr} - \frac{\omega^2 r}{g}\right) \tag{2}$$

where $K(=K^*\rho g)$ is the hydraulic conductivity in [$LT^{-1}$], $g$ is the gravitational acceleration [$LT^{-2}$] (i.e., 9.81 m $s^{-2}$) and $h$ is the pressure head [L].

[11] While the Richards equation in a unit gravitational field has the following formulation

$$\frac{\partial\theta}{\partial t} = \frac{\partial}{\partial x}\left[K\left(\frac{\partial h}{\partial x} + \cos\alpha\right)\right] \tag{3}$$

where $\theta$ is the water content [$L^3\,L^{-3}$], and $\alpha$ is the angle between gravity and flow direction (0° for vertical flow), the

modified version of the Richards equation for a centrifugal field is:

$$\frac{\partial \theta}{\partial t} = \frac{\partial}{\partial r}\left[K\left(\frac{\partial h}{\partial r} - \frac{\omega^2 r}{g}\right)\right] \quad (4)$$

### 2.2. Numerical Model

[12] The numerical model for flow in a centrifugal field was developed by modifying the Hydrus-1d code [*Šimůnek et al.*, 1998b]. The Richards equation (3) in Hydrus is solved numerically using a Galerkin type linear finite element method combined with a mass lumping scheme, leading to a numerical scheme equivalent to standard finite differences. Integration in time is achieved using an implicit (backward) finite difference scheme for both saturated and unsaturated conditions. The water content term is evaluated using the mass conservative method proposed by *Celia et al.* [1990] that leads to the set of nonlinear algebraic equations:

$$\frac{\theta_i^{j+1,k+1} - \theta_i^j}{\Delta t} = \frac{1}{\Delta x}\left(K_{i+1/2}^{j+1,k}\frac{h_{i+1}^{j+1,k+1} - h_i^{j+1,k+1}}{\Delta x_i} - K_{i-1/2}^{j+1,k}\frac{h_i^{j+1,k+1} - h_{i-1}^{j+1,k+1}}{\Delta x_{i-1}}\right) + \frac{K_{i+1/2}^{j+1,k} - K_{i-1/2}^{j+1,k}}{\Delta x}\cos\alpha \quad (5)$$

After taking into account initial and boundary conditions, these are solved using the Picard iteration scheme. In (5), $i$ is the node number in the spatial discretization, $j$ is the index for the temporal discretization, $k$ is the iteration number in the Picard iteration scheme, $\Delta t$ is the time step [T], and $\Delta x$ [$=(x_{i+1} - x_{i-1})/2$], $\Delta x_i$ [$=x_{i+1} - x_i$], and $\Delta x_{i-1}$ [$=x_i - x_{i-1}$] are spatial discretization steps [L].

[13] The modified Richards equation for flow in a centrifugal field (4) is discretized in a similar manner, leading to

$$\frac{\theta_i^{j+1,k+1} - \theta_i^j}{\Delta t} = \frac{1}{\Delta r}\left(K_{i+1/2}^{j+1,k}\frac{h_{i+1}^{j+1,k+1} - h_i^{j+1,k+1}}{\Delta r_i} - K_{i-1/2}^{j+1,k}\frac{h_i^{j+1,k+1} - h_{i-1}^{j+1,k+1}}{\Delta r_{i-1}}\right) - \frac{\omega^2}{g}\left(K_i^{j+1,k} + r_i\frac{K_{i+1/2}^{j+1,k} - K_{i-1/2}^{j+1,k}}{\Delta r}\right) \quad (6)$$

where $\Delta r$ [$=(r_{i+1} - r_{i-1})/2$], $\Delta r_i$ [$=r_{i+1} - r_i$], and $\Delta r_{i-1}$ [$=r_i - r_{i-1}$] are spatial discretization steps [L].

[14] Numerical solution requires adaptive time steps and spatially variable discretization. Discretization at the outflow boundary needs to be significantly finer to accommodate large gradients at early times after a change in the rotation speed and to result in small mass balance errors.

[15] Special attention needs to be paid to flux boundary conditions, since they have an important effect on stability of the numerical solution, as well as on the overall mass balance error. The upper boundary condition was specified by discretization of the Richards equation as follows:

$$\frac{\theta_N^{j+1,k+1} - \theta_N^j}{\Delta t} = \frac{2}{\Delta r_{N-1}}\left(-q_N^{j+1} - K_{N-1/2}^{j+1,k}\frac{h_N^{j+1,k+1} - h_{N-1}^{j+1,k+1}}{\Delta r_{N-1}} + K_{N-1/2}^{j+1,k}\frac{\omega^2 r_{N-1/2}}{g}\right) \quad (7)$$

while the lower boundary condition discretized Darcy's law:

$$q_1 = -K\left(\frac{dh}{dr} - \frac{\omega^2 r}{g}\right) \approx -K_{1+1/2}^{j+1,k}\left(\frac{h_2^{j+1,k+1} - h_1^{j+1,k+1}}{\Delta r} - \frac{\omega^2 r_{1+1/2}}{g}\right) \quad (8)$$

where $q_N$ and $q_1$ are the specified upper and lower boundary fluxes [$LT^{-1}$] and indices $N$ and 1 represent boundary nodes.

### 2.3. Soil Hydraulic Properties

[16] The unsaturated soil hydraulic properties in this paper are assumed to be represented by the following expressions [*van Genuchten*, 1980]:

$$S_e(h) = \frac{\theta(h) - \theta_r}{\theta_s - \theta_r} = \frac{1}{(1 + |\alpha h|^n)^m} \quad (9)$$

$$K(\theta) = K_s S_e^l\left[1 - \left(1 - S_e^{1/m}\right)^m\right]^2 \quad (10)$$

where $S_e$ is the effective water content (dimensionless), $K_s$ is the saturated hydraulic conductivity [$LT^{-1}$], $\theta_r$ and $\theta_s$ denote residual and saturated water contents [$L^3\ L^{-3}$], respectively, $l$ is a pore connectivity parameter (dimensionless), and $\alpha$ [$L^{-1}$], $n$ (dimensionless), and $m(=1 - 1/n)$ (dimensionless) are empirical parameters. The predictive $K(\theta)$ model is based on the capillary model of *Mualem* [1976] in conjunction with equation (9). The pore connectivity parameter $l$ in the hydraulic conductivity function was estimated by *Mualem* [1976] to be 0.5 as an average for many soils. The hydraulic characteristics defined by equations (9) and (10) contain 5 unknown parameters: $\theta_r$, $\theta_s$, $\alpha$, $n$, and $K_s$. For a multirotation experiment carried out as a drying process, the hydraulic parameters in Equations (9) and (10) represent drying branches of the unsaturated hydraulic properties.

### 2.4. Parameter Optimization

[17] The soil hydraulic parameters of (9) and (10) are obtained by calibrating the numerical model by minimizing the objective function $\Phi$ defined as the sum of squared deviations between measured and calculated water contents:

$$\Phi(\boldsymbol{b}, \theta) = \sum_{j=1}^{m}\sum_{i=1}^{n_j}\left[\theta_j^*(t_i) - \theta_j(t_i, \boldsymbol{b})\right]^2 \quad (11)$$

where $m$ represents different locations of water content measurements, $n_j$ is the number of measurements at a particular location, $\theta_j^*(t_i)$ are specific water content measurements at time $t_i$ and location $j$, and $\theta_j(t_i, \boldsymbol{b})$ are the corresponding model predictions for the vector of optimized parameters $\boldsymbol{b}$ (e.g., $\theta_r$, $\theta_s$, $\alpha$, $n$, and $K_s$).

[18] Minimization of the objective function $\Phi$ is accomplished by using the Levenberg-Marquardt nonlinear minimization method [*Marquardt*, 1963], which has become a commonly used approach in nonlinear least squares fitting among soil scientists and hydrologists [*Šimůnek and Hopmans*, 2002]. The method combines the Newton and steepest descend methods, and provides confidence intervals for the optimized parameters. Since the Levenberg-

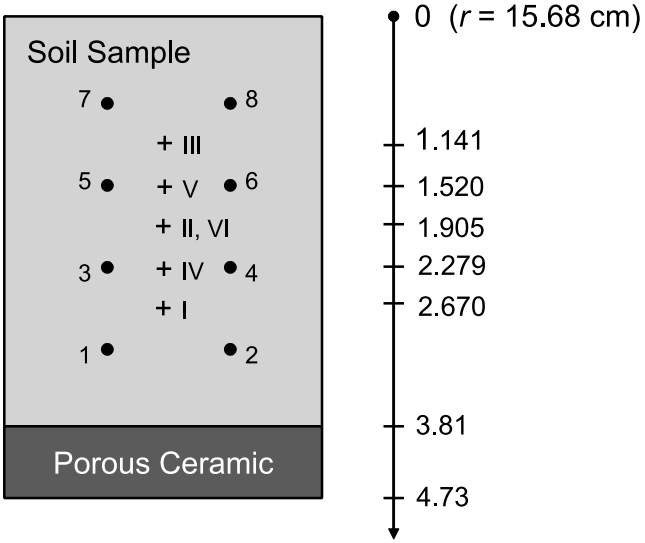


**Figure 1.** Schematic of the soil sample, location of electrodes (Arabic numberals), and assumed locations for water content measurements (Roman numerals). Water contents for location I were calculated by analyzing signal from electrodes 1, 2, 3, and 4. Similarly, location II corresponds to electrodes 3, 4, 5, and 6; location III corresponds to electrodes 5, 6, 7, and 8; location IV corresponds to electrodes 1, 2, 5, and 6; location V corresponds to electrodes 3, 4, 7, and 8; and location VI corresponds to electrodes 1, 2, 7, and 8. See color version of this figure in the HTML.

Marquardt method is a gradient method that seeks only the local minimum, we restarted each optimization with several different initial estimates of optimized parameters, and report here those that resulted in the lowest value of the objective function.

[19] Although in the presented analyses we assume that measured water contents are point measurements, the numerical code can also consider a finite measurement volume by averaging calculated water contents over specified volume. While in this paper we define the objective function only in terms of the water content, the Hydrus model allows other types of information, such as pressure heads and actual or cumulative outflow, to be considered as well.

## 3. Materials, Methods, and Data

[20] Details about the centrifuge apparatus, as well as about the soil sample used in this study are given by *Nimmo* [1990]. Here we only summarize the main features of completed experiments and their corresponding analyses. The centrifuge was specially modified by the manufacturer, Beckman Instruments, to incorporate a Meridian Laboratory MM12 high-speed, low-noise rotating electrical contractor on top of the rotor. (Brand names are given for identification only and do not indicate any endorsement by UCR or USGS.) The soil sample was placed in a retainer on a porous ceramic plate 9.2 mm thick (Figure 1). The effective hydraulic conductivity of a plate was measured to be $3 \times 10^{-7}$ m s$^{-1}$ [*Nimmo*, 1990]. A short lip of the impervious plate supporting the ceramic plate maintained a water table near the bottom of the ceramic plate (away from the axis of rotation). For different rotation speeds the water table at this position established different constant pressure heads at the outflow boundary of the soil sample.

[21] Eight electrodes in two vertical rows were installed through the retainer into the soil sample. This configuration allowed electrical conductivity measurements using six different four-electrode sets (Figure 1). Three main measurements were obtained by using four neighboring electrodes (small square configuration), and thus electrodes 1, 2, 3, and 4 composed the lower electrode set (measurements I); 3, 4, 5, and 6 the middle set (measurements II); and 5, 6, 7, and 8 the upper set (measurements III). Three other combinations of electrodes (larger rectangle configuration) could also be analyzed, resulting in measurement sets IV (electrodes 1, 2, 5, and 6), V (electrodes 3, 4, 7, and 8), and VI (electrodes 1, 2, 7, and 8). Electrical conductivity observations are thus at mean depths of 2.67, 1.905, 1.141, 2.279, 1.520, 1.905 cm for measurement sets I through VI. *Nimmo* [1990] conducted supplementary measurements showing that about 90% of the measurement influence is confined to a region within 9 mm of the center of each square. The published results of these supplementary measurements can be used in evaluating the uncertainty that results from assuming that data measured with the square electrode array represent point measurements at the center of each square. The calibration procedure to obtain water contents from measured electrical conductivity measurements is described by *Nimmo* [1990].

[22] Experiments were carried out on Oakley sand packed to a bulk density of 1.83 Mg/m$^3$ and porosity 0.333. The soil hydraulic properties, i.e., the hydraulic conductivities and retention data were measured using the steady state centrifuge method by *Nimmo and Akstin* [1988]. The soil sample had a height of 38 mm and a diameter of 25.4 mm. The soil was saturated before experimental runs using selenate solution (0.01 N $CaSO_4$ and 0.01 $CaSeO_4$) with electrical conductivity equal to 1.43 dS/m at the laboratory temperature of 22°C.

[23] The sequence of rotation speeds followed in three separate runs from resaturation is given in Table 1. Table 1 also indicates the centrifugal force for the applied rotation speed at the center of the soil sample. Note that in our

**Table 1.** Sequences of Centrifuge Speeds[a]

| Run 1 | | | Run 2 | | | Run 3 | | |
|---|---|---|---|---|---|---|---|---|
| $t$, s | $\omega$, s$^{-1}$ | $g$ | $t$, s | $\omega$, s$^{-1}$ | $g$ | $t$, s | $\omega$, s$^{-1}$ | $g$ |
| 10,249 | 46.1 | 38.1 | 5 | 50.3 | 45.5 | 10 | 6.3 | 0.71 |
| 64,129 | 57.6 | 59.5 | 40 | 33.8 | 20.5 | 15 | 50.3 | 45.5 |
| 72,353 | 70.2 | 88.3 | 65 | 24.1 | 10.4 | 40 | 45.0 | 36.4 |
| 80,352 | 74.3 | 99.2 | 90 | 16.8 | 5.1 | 60 | 35.6 | 22.8 |
| 92,299 | 104.7 | 197 | 4,389 | 14.7 | 3.9 | 6,393 | 29.3 | 15.4 |
| 144,744 | 136.1 | 333 | 9,028 | 22.0 | 8.7 | 10,345 | 33.5 | 20.2 |
| 169,222 | 230.4 | 953 | 13,737 | 29.3 | 15.4 | 17,825 | 36.7 | 24.1 |
| | | | 25,219 | 38.7 | 26.9 | 33,067 | 38.7 | 26.9 |
| | | | 75,879 | 46.1 | 38.1 | 83,677 | 41.9 | 31.5 |
| | | | 95,969 | 57.6 | 59.5 | 93,988 | 46.1 | 38.1 |
| | | | 115,576 | 104.7 | 197 | 104,234 | 52.4 | 49.2 |
| | | | | | | 122,717 | 57.6 | 59.5 |
| | | | | | | 379,884 | 70.1 | 88.3 |

[a]Here $t$, final time for given rotations; $\omega$, rotation speed (rad s$^{-1}$); $g$, multiple $g$ acceleration.

**Table 2.** Soil Hydraulic Parameters Obtained From Equilibrium Analyses[a]

| Run | $\theta_r$ | $\theta_s$ | $\alpha$, $m^{-1}$ | $n$ | $R^2$ |
|---|---|---|---|---|---|
| 1 | 0.047 (0.0023) | 0.280[b] | 3.28 (0.49) | 2.03 (0.11) | 0.94 |
| 2 | 0.00 | 0.280[b] | 19.6 (4.9) | 1.30 (0.029) | 0.82 |
| 3 | 0.015 (0.021) | 0.280[b] | 3.45 (0.38) | 1.76 (0.17) | 0.93 |
| 2a | 0.062 (0.0049) | 0.180 (0.0035) | 1.22 (0.082) | 3.45 (0.47) | 0.95 |
| 3a | 0.051 (0.011) | 0.200 (0.017) | 1.52 (0.26) | 2.65 (0.47) | 0.93 |

[a] $R^2$ is the regression coefficient. Standard errors are given in parentheses.
[b] Fixed.

calculations we could take into account not only the main time segments when a particular rotation speed was applied over a period of several hours, but also short time segments lasting only several seconds or minutes.

## 4. Results

[24] The collected experimental data can be analyzed in several ways. In the following sections we will first apply a simple equilibrium analysis and then the more complex inverse analyses using parameter estimation in combination with a numerical solver of the unsaturated flow equation.

### 4.1. Equilibrium Analyses

[25] First, we analyze measured water contents at the end of each main time segment, assuming that hydrostatic equilibrium was achieved before the next change of speed. We do realize that especially at greater rotation speeds, it is unlikely that the equilibrium conditions were fully reached. In the low-water-content conditions of these runs, however, $\theta$ is very weakly sensitive to $h$, so that deviations from equilibrium are minor, and thus errors from this assumption are minor as well. Numerical evaluation of equation (1) shows that equilibrium conditions are reached relatively quickly (within minutes) at low rotations, while at large rotation speeds the equilibration process can last many days [*Nimmo*, 1990] (see section 4.2).

[26] Under the assumption of equilibrium conditions, pressure heads for particular positions, $r$, can be calculated from [*Nimmo*, 1990]:

$$h(r) = \frac{\psi(r)}{\rho g} = \frac{\omega^2}{2g}\left(r^2 - r_0^2\right) \qquad (12)$$

where $r_0$ is the radius of location with zero potential [L] (=20.4 cm). These calculated pressure heads were then paired with corresponding measured water contents at the six locations I through VI (Figure 1) at the end of a particular time segment. The resulting retention data were fitted with the analytical model of *van Genuchten* [1980] using the RETC code [*van Genuchten et al.*, 1991]. Two sets of optimizations were done on each data set. First, we optimized three retention parameters $\theta_r$, $\alpha$, and $n$, and fixed the saturated water content $\theta_s$ to a value reported by *Nimmo* [1990]. Then we fitted all four retention parameters including $\theta_s$. The resulting soil hydraulic parameters for both optimizations are given in Table 2, while the graphs of both the measured retention data and their fits are shown in Figure 2. Note that since for the first run the first rotation speed was relatively high and thus the first retention data point was for the pressure head of $-80$ cm, we could not successfully fit the retention model without fixing the saturated water content. For the two other runs, with the first rotation speeds of 14.7 and 29.3 $s^{-1}$, the largest pressure heads were equal to $-9$ and $-35$ cm, respectively, and thus the retention curve was much better defined close to saturation, resulting in better fits. For run 2, however, measured water contents close to saturation for different locations display relatively large differences.

### 4.2. Transient Analyses

[27] Second, we analyzed transient data using parameter estimation in combination with a numerical solver of the unsaturated flow equation (1). Optimizations for each centrifugal run were again run in two sets. First, with all five soil hydraulic parameters optimized, and second with the effective saturated water content fixed at the observed value of 0.28 [*Nimmo*, 1990]. Figure 3 compares measured and fitted water contents for all three runs and for all 6 measurement locations. While measured water contents seem to be reaching the equilibrium state for slower speeds, as expected, for larger speeds water contents were still decreasing at the end of the run, and thus equilibrium was clearly not reached. In these cases, however, the measured water contents may not be significantly different from the values they would have at a true equilibrium state. Notice that there are significant differences in water contents within the soil sample at each speed, with the difference between the minimum and maximum water contents often larger

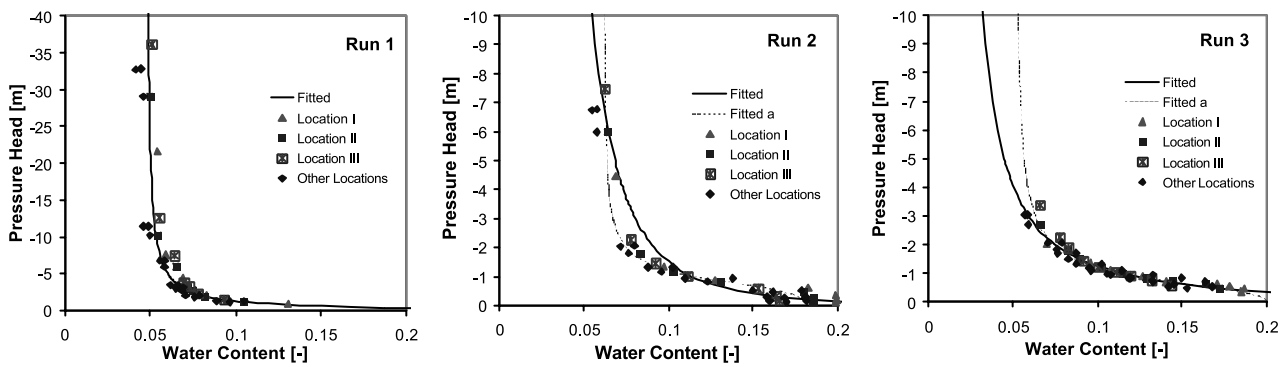


**Figure 2.** Retention curves resulting from the equilibrium analyses. The saturated water contents were either fixed (denoted Fitted) or fitted (Fitted a). See color version of this figure in the HTML.

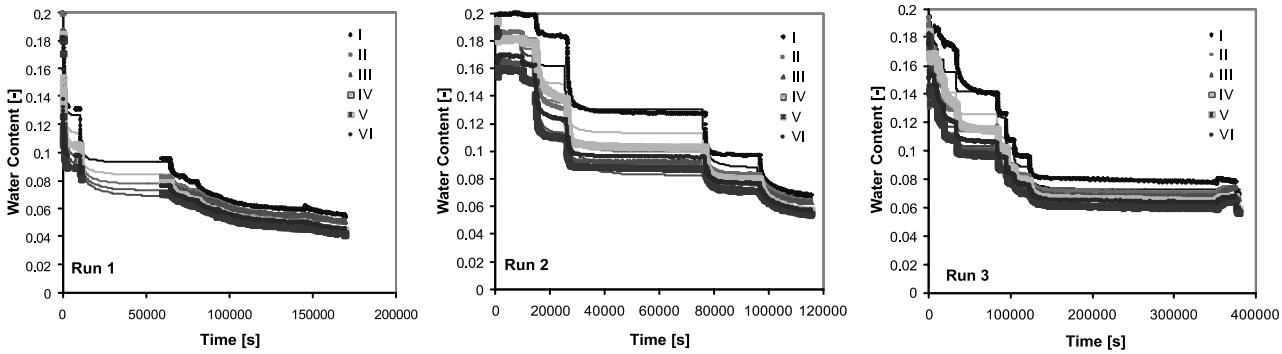


**Figure 3.** Measured and optimized water contents for three centrifuge runs 1, 2, and 3. See color version of this figure in the HTML.

than 0.05. That means that at each rotational speed the outflow experiment in a centrifugal field, especially at intermediate and larger speeds, provides more information than the similar experiment in the gravitational field (in which a much smaller range of water content is represented).

[28] The numerical model was relatively successful in describing the pattern in measured data, both the early stages of water content changes after the change in the rotational speed, as well as reaching of the equilibrium stage (Figure 3). Agreement is better for the measurements at higher speeds, consistent with the observation by *Nimmo* [1990] that various factors cause greater experimental uncertainty in the lower-speed data. The optimized soil hydraulic parameters and their standard errors are given in Table 3 together with regression coefficients of the fit.

## 5. Discussion

[29] Figure 4 shows calculated pressure head and water content profiles for all three runs at times when rotational speed was changed. A parabolic decrease of the pressure head from the bottom of the sample toward the top would represent an equilibrium status. The pressure head is expected to decrease parabolically within the porous ceramic, which is assumed to be fully saturated at all times; thus propagation of pressure should be relatively quick. Visually it seems that equilibrium pressure head profiles were not reached only for the last three rotational speeds for run 1 (the three largest speeds) (Figure 4a), and for the last two speeds for run 2 (Figure 4b), for which the duration was relatively short (Figure 3, middle). A large increase in rotational speed may lead to sudden desaturation of the bottom of the soil sample. Associated decrease of the hydraulic conductivity in the soil close to the interface may establish a significant resistance to draining of the sample and reaching of equilibrium conditions.

[30] The comparison of transient optimized retention functions with water contents obtained under the assumption of equilibrium state at the end of each rotation speed for all three runs is shown in Figure 5. Notice that there is a very good correspondence between optimized retention curves for intermediate pressure heads between $-0.5$ and about $-3$ m. There is a significant scatter of water content values close to saturation, probably caused by slightly different initial conditions due to air entrapment during resaturation. By applying substantial acceleration from the very beginning, little information is collected for the experimental range close to saturation. This experimental range is prone to large uncertainties even for experiments in the gravitational field [*Hopmans et al.*, 2002] and acceleration of the experiment in this range is usually not recommended [*Wendroth et al.*, 1993; *Šimůnek et al.*, 1998a]. Unless the saturation status is measured from the very beginning of the experiment or the mass balance information, such as the cumulative outflow, is collected (which was not the case for our experimental data), the fitted parameters that characterize the soil hydraulic properties close to saturation (that is, the saturated water content and the saturated hydraulic conductivity) are subject to large uncertainties. Since there are only very few water contents measurements with values above 0.2, the optimized soil hydraulic parameters are mainly determined by the soil hydraulic properties in the intermediate and dry saturation range. The saturated water content and the saturated hydraulic conductivity values should be viewed mainly as fitting parameters without clear physical meaning (see also *Schaap and Leij* [2000] and their discussion on the physical meaning of the fitted saturated hydraulic conductivity). Simultaneous fitting of these two

**Table 3.** Soil Hydraulic Parameters Obtained From Transient Analyses[a]

| Run | $\theta_r$ | $\theta_s$ | $\alpha$, $m^{-1}$ | $n$ | $K_s$, m $s^{-1}$ | $R^2$ |
|---|---|---|---|---|---|---|
| 1 | 0.043 (0.00052) | 0.220 (0.0025) | 1.76 (0.051) | 2.38 (0.038) | 7.30e-07 (6.10e-08) | 0.92 |
| 2 | 0.055 (0.00081) | 0.184 (0.00044) | 1.19 (0.0081) | 3.69 (0.063) | 1.00e-07 (6.0e-09) | 0.94 |
| 3 | 0.061 (0.00034) | 0.191 (0.00078) | 1.39 (0.010) | 3.38 (0.038) | 2.29e-07 (1.65e-08) | 0.96 |
| 1a | 0.040 (0.00065) | 0.280[b] | 2.07 (0.094) | 2.13 (0.032) | 3.87e-06 (1.8e-07) | 0.91 |
| 2a | 0.000 (0.0028) | 0.280[b] | 11.5 (0.30) | 1.39 (0.0082) | 2.31e-05 (2.5e-06) | 0.81 |
| 3a | 0.038 (0.001) | 0.280[b] | 3.14 (0.031) | 1.98 (0.017) | 1.01e-05 (5.2e-07) | 0.94 |

[a] $R^2$ is the regression coefficient. Standard errors are given in parentheses. Read 7.30e-07 as $7.30 \times 10^{-7}$.
[b] Fixed.

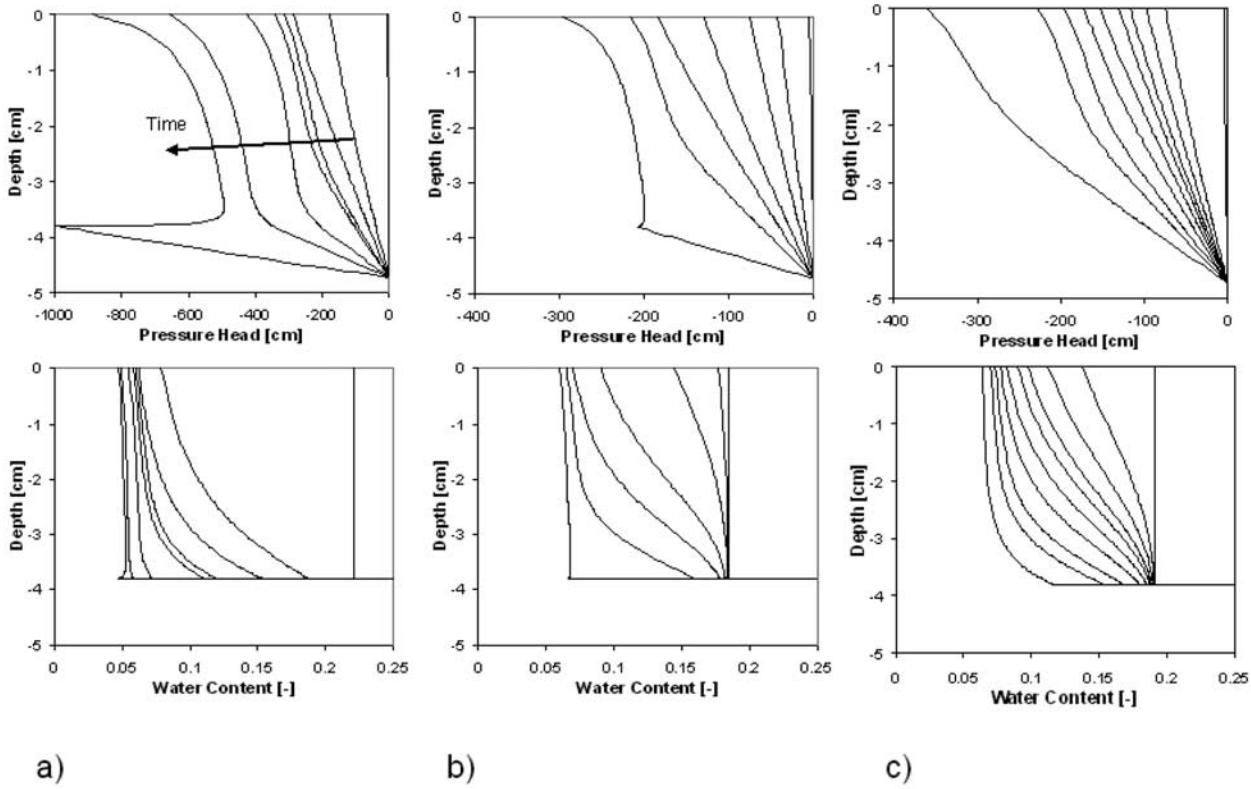


**Figure 4.** (top) Pressure heads and (bottom) water contents at times when rotation speed was changed: (a) run 1, (b) run 2, and (c) run 3. See color version of this figure in the HTML.

parameters together with the shape parameters, however, is recommended [*Hopmans et al.*, 2002] since it provides numerical code with additional flexibility to describe soil hydraulic properties in the measuring range for which most information is collected, i.e., intermediate and dry range.

[31] There are slight differences also at the dry end, where the optimization routine returned values of $\theta_r$ in the range of 0.043 and 0.061. In run 1, a much greater rotation speed was used for the last step (see Table 1), and thus much smaller pressure heads and water contents were registered in this experiment compared to other two runs. Consequently, while the optimization program for run 1 could use actual information about water contents and pressure heads in a relatively dry range, in the other two runs that used slower rotational speeds, the optimization program only extrapolated soil hydraulic properties in this range from measurement at higher-pressure heads.

[32] Figure 6 shows retention curves resulting from both the equilibrium and transient analyses. All retention curves are in a relatively narrow range. There are again larger differences in obtained retention curves only close to saturation and at the dry end. These differences are similar to those reported in Figure 5.

[33] Finally, Figure 7 shows comparison of hydraulic conductivity functions obtained using numerical inversion of transient centrifugal experiments and independently measured hydraulic conductivities using steady state centrifuge experiments [*Nimmo et al.*, 1987]. Figure 7 also shows the analytical function fitted to measured hydraulic conductivities by *Nimmo et al.* [1987]. Notice that all hydraulic conductivity functions pass in a relatively narrow range around measured values, and that they deviate significantly between themselves only for pressure heads for which there are no measurements. Extrapolation of optimized soil hydraulic functions beyond the range of measurements is usually expected to be associated with a high level of uncertainty [e.g., *Hopmans et al.*, 2002].

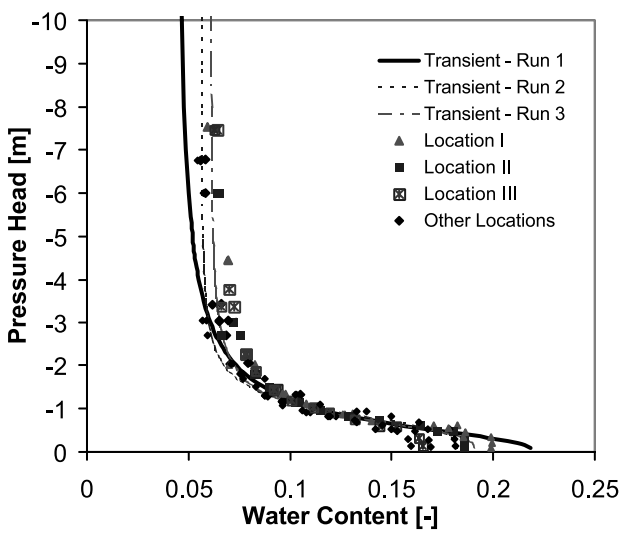


**Figure 5.** Optimized retention curves for three runs compared to water contents obtained assuming equilibrium at each time of change of rotational speed. See color version of this figure in the HTML.

Hydraulic conductivity functions fitted to transient centrifugal data show similar shapes and values.

## 6. Summary

[34] High-speed centrifuges have been often used during the last two decades to measure water retention, and saturated and unsaturated hydraulic conductivities [e.g., *Nimmo et al.*, 1987; *Conca and Wright*, 1992] of soil and rock samples. However, a steady state analysis is generally used to compute $K(\theta)$ from the measurements. Recent advances in centrifuge experiments allow measurements of multiple transient variables, such as pressure heads, water contents, concentrations, and outflow rates during the experiment, i.e., variables that can be used to advantage with parameter estimation techniques.

[35] In this paper we presented a modified version of the Hydrus software package that can directly or inversely simulate water flow in a centrifugal field, and the application of this new model to previously published data of *Nimmo* [1990]. Using time-variable water contents measured at a sequence of several rotational speeds, we successfully estimated soil hydraulic properties by numerical inversion of transient experiments. The optimized soil hydraulic properties compared well with those determined using equilibrium analysis and steady state experiments.

[36] Similar parameter estimation procedures are often used in soil physics for analyzing one-step and multistep outflow experiments [*Hopmans et al.*, 2002]. Multirotation experiments in a centrifuge not only offer significant time savings by accelerating time, but also provide significantly more information for the parameter estimation procedure. Multistep outflow experiments in a gravitational field, if carried out for a sufficiently long time to reach steady conditions, provide a single pair of the water content and pressure head at each pressure step that defines one data point of the retention curve. Multirotation experiments, on the other hand, can provide multiple pairs of pressure heads and water contents for a single rotational speed. This is because the pressure head changes significantly between the bottom and the top of the sample in a centrifugal field, while it is almost uniform for the multistep experiment in a gravitational field. The advantage of collecting multiple retention data points at one speed is partly overcome by increasing nonlinearity of water content distribution within a measurement window over which the water content is averaged compared to the usual gravity system. In transient conditions a wide range of pressure heads also occurs for multistep outflow experiments and these pressure heads can be measured with tensiometers and used in the inverse analyses. A detailed sensitivity analyses on both measured and synthetic data, however, would then be required to reveal which experiment provides more information and is more reliable to determine soil hydraulic properties. It seems plausible that if multirotation experiments are carried out for a sufficiently long time at each rotational speed to reach steady conditions, the collected data can provide multiple points of the retention curve that would warrant the optimization of free form analytical functions such as those suggested by *Bitterlich et al.* [2004].

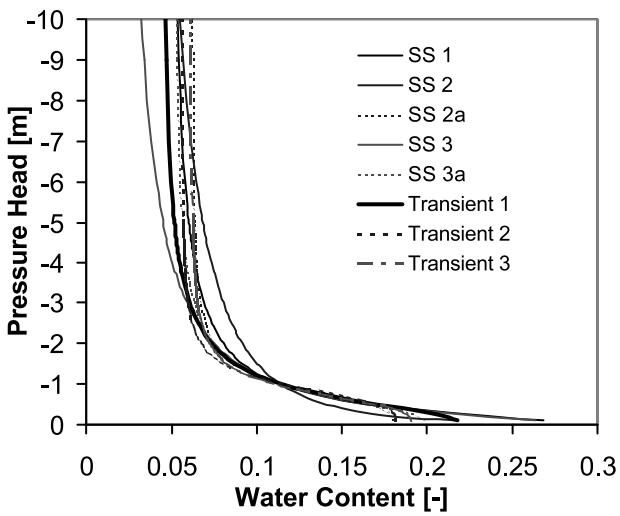


**Figure 6.** Retention curves resulting from the equilibrium (SS) and transient (Transient) analyses. Number in the legend refers to run number. See color version of this figure in the HTML.

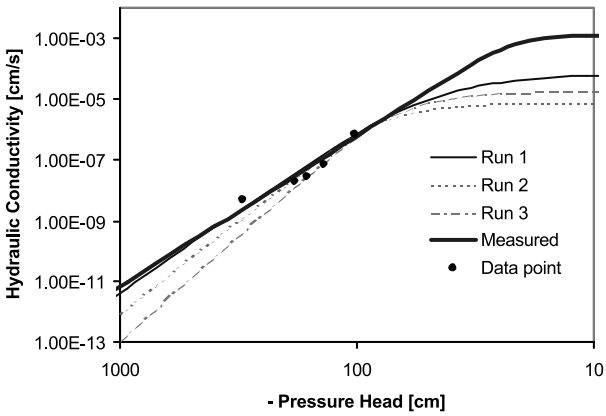


**Figure 7.** Hydraulic conductivity functions obtained using the parameter estimation analyses of transient centrifugal experiments and hydraulic conductivities measured using steady state analyses [*Nimmo et al.*, 1987]. The thick solid line was fitted to measured data obtained from steady state experiments. See color version of this figure in the HTML.

[37] **Acknowledgment.** The senior author would like to thank Earl Mattson and Carl Palmer from Idaho National Laboratory for providing funding to develop the numerical solver for the centrifugal conditions.

## References

Alemi, M. H., D. R. Nielsen, and J. W. Biggar (1976), Determining the hydraulic conductivity of soil cores by centrifugation, *Soil Sci. Soc. Am. J.*, *40*, 212–218.

Bear, J., M. Y. Corapcioglu, and J. Balakrishna (1984), Modeling of centrifugal filtration in unsaturated deformable porous media, *Adv. Water Resour.*, *7*, 150–167.

Bitterlich, S., W. Durner, S. C. Iden, and P. Knabner (2004), Inverse estimation of the unsaturated soil hydraulic properties from column outflow experiments using free-form parameterizations, *Vadose Zone J.*, *3*, 971–981.

Briggs, L. J., and J. W. McLane (1907), The moisture equivalent of soils, *U.S. Bur. Soils Bull.*, *45*, 23 pp.

Celia, M. A., E. T. Bououtas, and R. L. Zarba (1990), A general mass-conservative numerical solution for the unsaturated flow equation, *Water Resour. Res.*, *26*, 1483–1496.

Conca, J. L., and J. Wright (1992), A new technology for direct measurements of unsaturated transport, paper presented at the Nuclear and

Hazardous Waste Management Spectrum '92 Meeting, An. Nucl. Soc., Boise, Idaho.

Conca, J. L., and J. A. Wright (1998), The UFA method for rapid, direct measurement of unsaturated transport properties in soil, sediment, and rock, *Aust. J. Soil Res.*, *36*, 291–315.

Culligan, P. J., D. A. Barry, and J. Y. Parlange (1997), Scaling unstable infiltration in the vadose zone, *Can. Geotech. J.*, *34*(3), 466–470.

Dane, J. H., and J. W. Hopmans (2002), Hanging water column, in *Methods of Soil Analysis*, part 4, *Physical Methods*, edited by J. H. Dane and G. C. Topp, pp. 680–683, Soil Sci. Soc. of Am., Madison, Wis.

Dane, J. H., and G. C. Topp (Eds.) (2002), *Methods of Soil Analysis*, part 1, *Physical Methods*, 3rd ed., Soil Sci. Soc. of Am., Madison, Wis.

Durner, W., E. B. Schultze, and T. Zurühl (1999), State-of-the-art in inverse modeling of inflow/outflow experiments, in *Characterization and Measurement of the Hydraulic Properties of Unsaturated Porous Media*, edited by M. T. van Genuchten et al., pp. 661–681, Univ. of Calif., Riverside.

Eching, S. O., and J. W. Hopmans (1993), Optimization of hydraulic functions from transient outflow and soil water pressure data, *Soil Sci. Soc. Am. J.*, *57*, 1167–1175.

Forbes, P. L. (1994), Simple and accurate methods for converting centrifuge data into drainage and imbibition capillary pressure curves, *Log Anal.*, *35*, 31–53.

Gardner, R. (1937), A method of measuring the capillary tension of soil moisture over a wide moisture range, *Soil Sci.*, *43*, 277–283.

Gardner, W. R. (1956), Calculation of capillary conductivity from pressure plate outflow data, *Soil Sci. Soc. Am. Proc.*, *20*, 317–320.

Griffioen, J. W., P. J. Culligan, D. A. Barry, and K. Banno (1997), Centrifuge scaling of unstable infiltration, *Recent Res. Dev. Soil Sci.*, *1*, 29–41.

Hassler, G. L., and E. Brunner (1945), Measurement of capillary pressures in small core samples, *Trans. Am. Inst. Min. Metall. Pet. Eng.*, *160*, 114–123.

Hopmans, J. W., J. Šimůnek, N. Romano, and W. Durner (2002), Inverse modeling of transient water flow, in *Methods of Soil Analysis*, part 1, *Physical Methods*, edited by J. H. Dane and G. C. Topp, pp. 963–1008, 3rd ed., Soil Sci. Soc. of Am., Madison, Wis.

Kool, J. B., J. C. Parker, and M. T. van Genuchten (1985), Determining soil hydraulic properties from one-step outflow experiments by parameter estimation: I. Theory and numerical studies, *Soil Sci. Soc. Am. J.*, *49*, 1348–1354.

Marquardt, D. W. (1963), An algorithm for least-squares estimation of nonlinear parameters, *SIAM J. Appl. Math.*, *11*, 431–441.

Mattson, E. D., K. E. Baker, C. D. Palmer, R. W. Smith, and J. Šimůnek (2003), One-dimensional solute transport in variably saturated soil using a geocentrifuge apparatus, *Eos Trans. AGU*, *84*(46), Fall Meet. Suppl., Abstract H22A-0906.

Mualem, Y. (1976), A new model for predicting the hydraulic conductivity of unsaturated porous media, *Water Resour. Res.*, *12*, 513–522.

Nakajima, H., E. D. Mattson, and A. T. Stadler (2003), Unsaturated hydraulic properties determined from geocentrifuge tests, *Eos Trans. AGU*, *84*(46), Fall Meet. Suppl., Abstract H22A-0908.

Nimmo, R. J. (1990), Experimental testing of transient unsaturated flow theory at low water content in a centrifugal field, *Water Resour. Res.*, *26*(9), 1951–1960.

Nimmo, J. R., and K. C. Akstin (1988), Hydraulic conductivity of a sandy soil at low water content after compaction by various methods, *Soil Sci. Soc. Am. J.*, *52*, 303–310.

Nimmo, R. J., and K. A. Mello (1991), Centrifugal techniques for measuring saturated hydraulic conductivity, *Water Resour. Res.*, *27*(6), 1263–1269.

Nimmo, J. R., J. Rubin, and D. P. Hammermeister (1987), Unsaturated flow in a centrifugal field: Measurement of hydraulic conductivity and testing of Darcy's law, *Water Resour. Res.*, *23*(1), 124–137.

Nimmo, J. R., K. S. Perkins, and A. M. Lewis (2002), Steady-state centrifuge, in *Methods of Soil Analysis*, part 1, *Physical Methods*, 3rd ed., edited by J. H. Dane and G. C. Topp, pp. 903–916, Soil Sci. Soc. of Am., Madison, Wis.

Paningbatan, E. P. (1980), Determination of soil moisture characteristic and hydraulic conductivity using a centrifuge, Ph.D. thesis, Univ. of Calif., Davis.

Russell, M. B., and L. A. Richards (1938), The determination of soil moisture energy relations by centrifugation, *Soil Sci. Soc. Am. Proc.*, *3*, 65–69.

Savvidou, C., and P. J. Culligan (1998), The application of centrifuge modeling to geo-environmental problems, *Proc. Inst. Civ. Eng. Geotech. Eng.*, *131*, 152–162.

Schaap, M. G., and F. J. Leij (2000), Improved prediction of unsaturated hydraulic conductivity with the Mualem–van Genuchten model, *Soil Sci. Soc. Am. J.*, *64*, 843–851.

Sigda, J. M., and J. L. Wilson (2003), Are faults preferential flow paths through semiarid and arid vadose zones?, *Water Resour. Res.*, *39*(8), 1225, doi:10.1029/2002WR001406.

Šimůnek, J., and J. W. Hopmans (2002), Parameter optimization and nonlinear fitting, in *Methods of Soil Analysis*, part 1, *Physical Methods*, 3rd ed., edited by J. H. Dane and G. C. Topp, pp. 139–157, Soil Sci. Soc. of Am., Madison, Wis.

Šimůnek, J., O. Wendroth, and M. T. van Genuchten (1998a), A parameter estimation analysis of the evaporation method for determining soil hydraulic properties, *Soil Sci. Soc. Am. J.*, *62*, 894–905.

Šimůnek, J., M. Šejna, and M. T. van Genuchten (1998b), The HYDRUS-1D software package for simulating the one-dimensional movement of water, heat, and multiple solutes in variably-saturated media, version 2.0, *Rep. IGWMC-TPS-70*, 202 pp., Int. Ground Water Model. Cent., Colo. Sch. of Mines, Golden, Colo.

van Dam, J. C., J. N. M. Stricker, and P. Droogers (1994), Inverse method to determine soil hydraulic functions from multistep outflow experiment, *Soil Sci. Soc. Am. J.*, *58*, 647–652.

van Genuchten, M. T. (1980), A closed-form equation for predicting the hydraulic conductivity of unsaturated soils, *Soil Sci. Soc. Am. J.*, *44*, 892–898.

van Genuchten, M. T., F. J. Leij, and S. R. Yates (1991), The RETC code for quantifying the hydraulic functions of unsaturated soils, *Rep. EPA/600/2-91-065*, U.S. Enviorn. Prot. Agency, Washington, D. C.

Wendroth, O., W. Ehlers, J. W. Hopmans, H. Kage, J. Halbertsma, and J. H. M. Wösten (1993), Reevaluation of the evaporation method for determining hydraulic functions in unsaturated soils, *Soil Sci. Soc. Am. J.*, *57*, 1436–1443.

J. R. Nimmo, U.S. Geological Survey, 345 Middlefield Road, MS-421, Menlo Park, CA 94025, USA. (jrnimmo@usgs.gov)

J. Šimůnek, Department of Environmental Sciences, University of California Riverside, Riverside, CA 92521, USA. (jiri.simunek@ucr.edu)